arXiv:2609.03584v1 [cs.SD] 3 Sep 2026

LOCAL CHORD CORRUPTION IS NOT RECOGNIZER REPLAY: CHORD-CONDITION PROPAGATION IN MIDI-SAG

Weiwen Huang

Shenzhen University
2510043030@mails.szu.edu.cn

ABSTRACT

Synthetic chord corruption provides a controlled stress test for singing accompaniment generation (SAG), whereas complete automatic chord recognition (ACR) replay measures the condition delivered to a deployed system. We compare them by replaying CNN–CRF and DeepChroma+CRF predictions through one fixed MIDI-SAG generator, holding track, seed, context, and scoring window constant. Across 30 paired tracks and three seeds, a central four-second tritone produced larger changed-target and inside-output effects than CNN–CRF replay in STFT, CQT, and CENS; the CENS target gap was positive on 29/30 tracks (mean 0.462). Matching replay support and relation composition reduced this mismatch, with joint matching giving the lowest replay distance in the full-30 analysis. Relative-root substitutions produced 2.88-fold larger CENS full-window output change than same-root quality flips at near-equal dose. The matched surrogate was closer to replay for both recognizer paths. We conclude that localized corruption tests mechanisms, whereas complete replay evaluates deployed chord-condition propagation.

Index Terms— singing accompaniment generation, automatic chord recognition, music generation, robustness evaluation, counterfactual analysis

1. INTRODUCTION

SAG creates instrumental backing from vocals. Audio-conditioned systems include SingSong and FastSAG [1, 2]; MIDI-Informed Singing Accompaniment Generation (MIDI-SAG) also exposes melody, chord, and MIDI controls [3]. When these controls are estimated, the analyzer becomes part of the generation system.

Short synthetic corruption is easy to align and reproduce, yet one concentrated edit cannot stand in for a full ACR sequence. ACR output mixes root, quality, and no-chord events with nonuniform temporal support. Thus, a robustness conclusion can change with the chord-condition test that is chosen. Existing work establishes chord-conditioned generation and robustness [4, 3]. Here we ask whether a prescribed local edit represents the complete recognizer-derived control sequence seen by a generator under matched conditions.

This distinction changes the meaning of a robustness result. A central corruption tests the response to one deliberately concentrated relation. Complete replay tests the response to the heterogeneous chord stream that an analysis front end actually delivers. These are complementary interventions, not interchangeable versions of the same test. Our paired design places them on the same track, context, seed, and scoring window so their output consequences can be compared directly.

We make three contributions. First, we introduce a paired chord-condition propagation protocol that fixes track, seed, context, prompt, scoring window, and generator while contrasting a local edit with a complete recognizer-derived sequence. Second, central and support/profile-matched edits show that a central tritone produces larger transfer effects than complete replay, while changed support and relation composition each remove most of the mismatch and their joint construction has the lowest replay distance. Third, this calibration direction holds across CNN–CRF and DeepChroma+CRF, two ACR paths replayed through the fixed MIDI-SAG generator.

2. RELATED WORK

SAG spans audio-only and explicitly conditioned generation [1, 2, 3]. AnyAccomp uses a quantized melodic bottleneck rather than a time-aligned chord interface [5]; the present intervention requires the latter.

Broader controllable-music systems provide melodic, textual, and time-varying control pathways [6, 7, 8, 9]; MusicGen-Chord adds chord-progressions to the MusicGen family [10, 11]. Gao et al. study robustness of chord-conditioned song generation to inaccurate chord extraction [4]. Their generator-centered question is whether a model tolerates imperfect control. Our evaluation-centered question is whether a localized synthetic condition represents the complete recognizer-derived chord sequence delivered to a fixed generator under matched rendering conditions.

ACR represents root, bass, quality, and duration; timing and label ambiguity are central evaluation issues [12, 13, 14, 15]. Related substitutions also differ musically [16, 17, 18]. CNN–CRF and DeepChroma+CRF provide distinct ACR paths [19, 20, 21]. We treat their complete outputs as deployed chord conditions. Their downstream consequences reflect label relation, temporal placement, and duration. This motivates an evaluation protocol for chord-condition propagation.

3. PAIRED CHORD-CONDITION PROPAGATION

3.1. Paired conditions

Let $G(v, c; s)$ generate accompaniment from vocals v, chord sequence c, and seed s. The baseline is $y_0 = G(v, c_0; s)$, where c_0 is MIDI-SAG's frozen time-aligned harmonization condition, not an expert reference [3]. CNN–CRF replay uses its full-song prediction c_r; the synthetic condition uses a frozen central four-second corruption c_s. Only c varies within pairs.

3.2. Chord-condition-propagation metrics

For each pair, x_t is the baseline accompaniment feature and y_t is the feature generated under the altered chord condition. Their

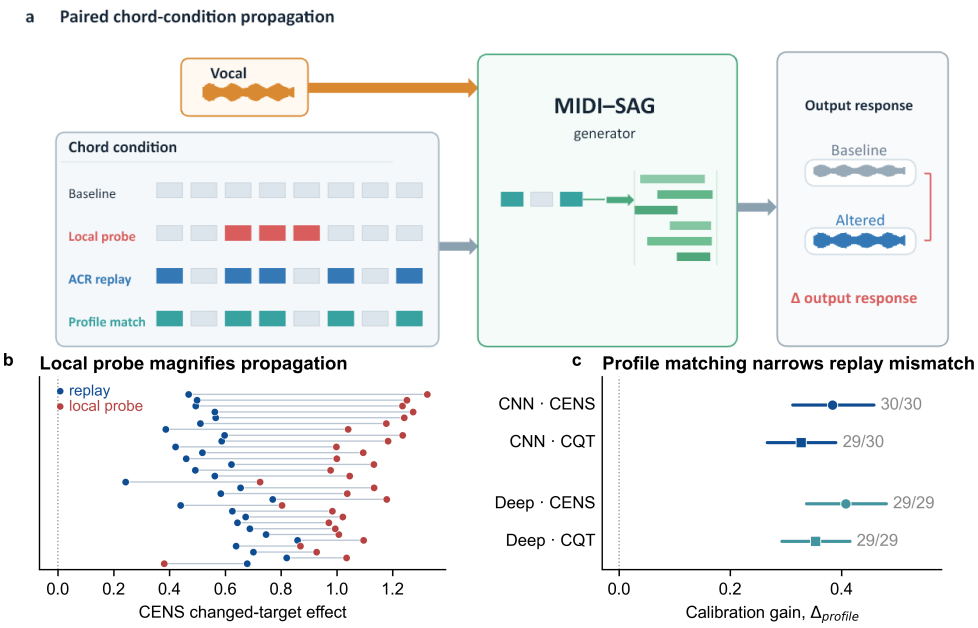

Fig. 1. Chord-condition propagation evidence. (a) The protocol holds the vocal track, seed, generator context, and scoring window fixed while varying the chord condition. (b) Three-seed CENS means for 30 paired tracks: the central tritone exceeds complete CNN–CRF replay on 29. (c) A surrogate that matches changed-block support and relation composition is closer to replay across two recognizer paths and two feature views, with the generator checkpoint held fixed. CNN denotes CNN–CRF and Deep denotes DeepChroma+CRF. Small points are tracks and large symbols are means.

chord templates are $h_0(t)$ and $h_1(t)$, respectively. All features use 0.5-s blocks and are ℓ_2-normalized before cosine comparison. The changed-target effect measures whether the altered-condition accompaniment moves toward its altered chord target:

$$E_{\text{target}} = \underset{t\in\mathcal{I}}{\text{mean}}\big\{\cos(y_t, h_1(t)) - \cos(y_t, h_0(t)) - \cos(x_t, h_1(t)) + \cos(x_t, h_0(t))\big\}. \tag{1}$$

where $\mathcal{I}$ is the changed-block set. Positive E_{target} therefore means that the altered output gained relative similarity to h_1 over h_0, beyond the baseline feature difference. Each condition has its own h_1, so the endpoint is condition-specific and may exceed one. The complementary inside-output change is the mean changed-block distance between x_t and y_t and introduces no target template. Full-window output change is the same distance averaged over the entire 12-s scoring window. Table 2 reports both endpoints in short-time Fourier transform (STFT) chroma, constant-Q transform (CQT), and chroma energy normalized statistics (CENS) [22, 23]; we average seeds within track before inference.

4. EXPERIMENTAL PROTOCOL

4.1. Data and generation

We froze 30 paired 12-s windows from 4,102 candidates in a 34-track evaluation pool before generation. Candidates were ranked by vocal activity, onset density, voiced RMS, and silence, then balanced across register and harmonic-change cells. Each 47.554-s MIDI-SAG context was fixed, CNN–CRF was run on the complete mixture and clipped to context, and only the chord condition varied within a pair [24]. We used seeds 42, 123, and 2027; all 180 central-probe and replay renders passed integrity checks.

Table 1. Complete CNN–CRF replay is root-change dominated: root-changing events account for 76.12% of scored event mass, while tritone substitutions account for 1.79%.

Category	Share	Category	Share
Other root	33.82%	Fifth root	24.60%
Agreement	16.03%	Relative root	11.40%
No-chord	4.45%	Semitone root	4.51%
Quality	3.41%	Tritone root	1.79%

Complete replay is dominated by root-changing events (76.12% of event mass; Table 1), whereas tritone substitutions account for only 1.79%. Other-root and fifth-root changes alone account for 33.82% and 24.60%, respectively. On the 0.5-s audit grid, their changed-block shares are 39.87% and 30.23%. We retain root, quality, no-chord, and agreement events as separate classes because they impose different harmonic conditions. Root changes alter pitch-class function, quality changes preserve the root, and no-chord events remove the harmonic target.

Track is the unit of inference. We average three seeds, form 95% bootstrap intervals from 10,000 track-level resamples, and use paired two-sided Wilcoxon tests with family-wise correction. The central edit spans four seconds, whereas CNN–CRF disagreement occupies 10.73 s on average.

Recognizer segments preserve their original boundaries in the frozen context and map into MIDI-SAG's root-plus-quality chord vocabulary. Profiles copy replay's changed-block mask and relation counts without copying its labels. Versioned manifests, metric tables, evaluators, and figure scripts make the paired results repro-

Table 2. Central four-second corruption magnifies both primary chord-condition-propagation endpoints relative to complete CNN–CRF replay across all three feature views (30-track means). Replay disagreement averaged 10.73 s; all six paired contrasts remained significant after BH correction ($q \leq 3.05 \times 10^{-5}$).

	E_{target}		Inside output	
View	4-s tri.	ACR replay	4-s tri.	ACR replay
STFT	0.268	0.167	0.105	0.081
CQT	0.902	0.505	0.526	0.421
CENS	1.045	0.583	0.598	0.451

ducible; the release package documents the complete mapping and audio-QA procedure.

4.2. Structure and specificity controls

An 18-track separate diagnostic compares a four-second relative root-changing substitution with a same-root quality flip at near-equal input-disagreement mass (0.1059 versus 0.1070); three seeds yield 108 renders. These tracks are held out from the 30-track confirmatory contrasts, but are not used in the primary transfer comparison.

On a nested 12-track subset, a block-occupancy control replaces exactly the CNN–CRF-changed 0.5-s blocks with a fixed fifth-root shift. It matches temporal support, not chord identity or input distance.

4.3. Profile-matched synthetic calibration

For each confirmatory track, three independently keyed profiles preserve baseline context, use CNN–CRF's exact changed-block mask, and match its scored-window relation-category counts without copying its labels. We compare their mean with central tritone and replay using

$$\Delta_{\text{profile}} = |E_{\text{central}} - E_{\text{replay}}| - |E_{\text{profile}} - E_{\text{replay}}|, \quad (2)$$

where positive values favor the support-and-profile-matched surrogate. CENS is the primary calibration view and CQT is its paired secondary view; all 270 profile renders passed audio QA.

We repeat calibration with DeepChroma+CRF predictions decoded from the same complete mixtures on 29 eligible tracks (87 replays and 261 profiles). This extends the calibration comparison to a second recognizer path. We then compare four constructions on the frozen CNN–CRF pairing: exact-mask-only uses replay support with a fixed fifth-root replacement, composition-only uses central support with replay relation counts, and the existing full profile matches both. The 360 new renders retain context, prompt, window, and seed; this is a separate diagnostic construction family.

All profile renders passed integrity checks. Construction contrasts isolate the contribution of matched support and relation composition to replay fidelity.

5. RESULTS

5.1. Central corruption magnifies condition propagation

Synthetic corruption produced larger measured changed-target and inside-output effects than CNN–CRF replay in every representation (Table 2). The CENS target gap was positive on 29/30 tracks (mean 0.462, 95% CI $[0.377, 0.539]$, $p = 2.61 \times 10^{-8}$); inside-output was positive on 28/30 (mean 0.146, CI $[0.110, 0.180]$, $p = 5.72 \times 10^{-7}$). All six frozen tests survived BH correction ($q \leq 3.05 \times 10^{-5}$). The central probe thus yielded a larger response even though complete replay occupied more than twice as much of the scored window.

The gap was not driven by one diffusion realization. Seed-specific CENS means were 0.468, 0.469, and 0.450; each seed was positive on 29/30 tracks, and track ranks correlated 0.76–0.77 across seed pairs. We average seeds within track for inference.

5.2. Relative-root changes induce stronger propagation than quality flips

Relative root-changing substitutions transferred more strongly than same-root quality flips in all representations. In CENS, the relative-root effect was larger on all 18 diagnostic tracks (2.88-fold mean full-window output change; $p = 7.6 \times 10^{-6}$; Fig. 2a), with a paired changed-target advantage of 0.251 (CI $[0.208, 0.292]$). STFT/CQT ratios were 1.89/3.41. The frozen chord encoder also separated these conditions (distance 0.004085 versus 0.002932).

The held-out relation control matches symbolic disagreement mass (0.1059 versus 0.1070), showing that the effect follows chord relation rather than perturbation dose.

5.3. Support matching recovers much of the replay response

The occupancy control matched changed duration exactly (mean 10.75 s) and had similar input distance to replay (0.639 versus 0.599, $p = .339$). Its STFT target effect matched replay (0.166 versus 0.178, $p = .622$), while CQT/CENS target differences were $-0.076/-0.069$ and CENS inside-output remained lower (-0.047,

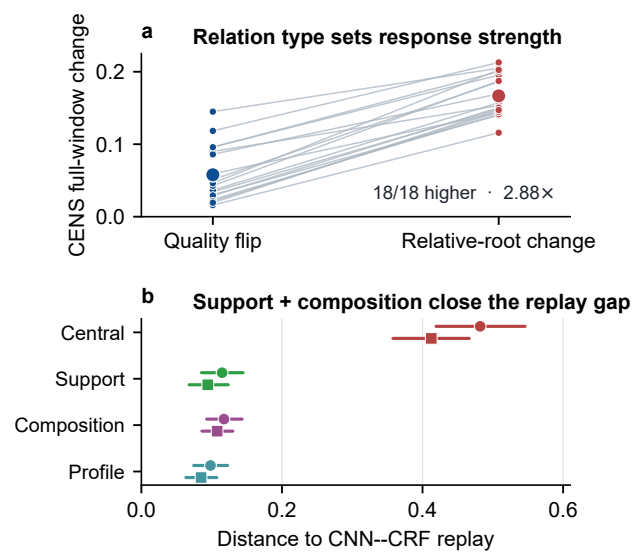

Fig. 2. Mechanism and calibration diagnostics. (a) Four-second relative-root substitutions exceed same-root quality flips in CENS full-window output change on all 18 diagnostic tracks at near-equal symbolic mass; large points are means. (b) Matching either replay support (exact mask) or relation composition sharply reduces central-probe distance, while the joint profile has the lowest mean replay distance. Circles and squares show CENS and CQT means with 95% track-bootstrap intervals.

CI $[-0.084, -0.013]$, $p = .027$). Matching temporal occupancy recovers a substantial part of replay transfer. The remaining gap is attributable to relation composition: exact-window other-root share tracked CQT/CENS changed-target effects after controlling input mass ($\rho = 0.600/0.589$, globally corrected $q = 0.025$).

5.4. Profile matching resolves the synthetic–replay mismatch

The support-and-profile construction was closer to CNN–CRF replay than the central tritone (Fig. 1c): CENS was positive on all 30 tracks (mean 0.384, CI $[0.314, 0.457]$, $p = 1.86 \times 10^{-9}$); CQT was positive on 29/30 (mean 0.328, CI $[0.268, 0.390]$, $p = 3.73 \times 10^{-9}$). The same direction reappeared on all 29 eligible DeepChroma+CRF tracks, with CENS/CQT gains of $0.408/0.353$ ($p = 3.73 \times 10^{-9}$ for both).

Profile matching also produces lower changed-block output distance without a target template (CENS/CQT gains 0.122/0.080; 28/30 and 24/30 tracks; both exact $p < 4.5 \times 10^{-6}$). The same direction on target-following and target-independent endpoints shows that calibration is a property of the output response, not one scoring template.

The full-30 construction analysis shows that changed support and relation composition are both key profile coordinates: mean CENS replay distances were 0.482 (central), 0.115 (exact mask), 0.117 (composition only), and 0.098 (full); CQT gave 0.412, 0.094, 0.108, and 0.085. Exact support reduced central distance on 28/30 tracks in both views (gains 0.367 and 0.318; Holm-adjusted $p < 2 \times 10^{-7}$). Composition at central support also reduced it on 29/30 and 28/30 tracks (0.364 and 0.305; Holm-adjusted $p < 7 \times 10^{-8}$). The joint profile had the lowest mean distance (0.098/0.085), with additional mean reductions of 0.016/0.010 over exact-mask-only and 0.019/0.023 over composition-only (CENS/CQT). Together, these results establish changed support and relation composition as the two key coordinates for replay-matched synthetic evaluation.

The condition audit exposes the geometry of each construction. Central and composition-only probes change 4.03 s; exact-mask, full-profile, and replay conditions change 10.03 s. Changed-block raw-template distance is 0.991 for central, 0.658 for composition-only, 0.649 for exact-mask, 0.650 for full-profile, and 0.592 for replay. Frozen chord-CNN distance is 0.111, 0.071, 0.064, 0.072, and 0.068, respectively. This audit makes the geometry behind each construction visible; target-independent output distance confirms the same calibration pattern.

6. DISCUSSION

6.1. Implications for evaluation

A central four-second corruption and a complete recognizer-derived condition are not interchangeable transfer tests. Central corruption magnified the condition-propagation response on 29/30 tracks, whereas profile matching sharply narrowed replay distance on target-following and target-independent endpoints. The full-30 construction analysis identifies changed support and relation composition as the two coordinates that make a synthetic probe replay-like.

The result also clarifies the role of local intervention. Relative-root changes produced 2.88 times the CENS full-window output change of quality flips at near-equal dose. A localized edit is therefore a precise harmonic-mechanism test; complete replay is the operating-condition test. Both should be reported, but they should not be merged into a single robustness score.

CNN–CRF and DeepChroma+CRF use different acoustic front ends, yet profile matching improves replay fidelity for both. This consistency shows that the evaluation rule is stable across recognizer paths in the MIDI-SAG conditioner.

The factor analysis further shows why a single chord-error rate is not enough for SAG evaluation. Two control streams can contain comparable amounts of disagreement but drive different accompaniment responses when their changed regions or chord relations differ. Error structure is therefore part of the condition presented to the generator. Support records when the control changes; relation composition records what musical substitutions it contains. Reporting these coordinates makes the gap between a convenient stress test and a deployed recognizer stream visible.

6.2. Practical protocol

Freeze the vocal excerpt, generator context, prompt, seed, and scoring window; render the baseline and complete recognizer sequence; then score their paired output change. Add a localized chord edit only when testing a named harmonic mechanism. Reporting the local response beside replay distance reveals whether a claimed robustness gain reflects sensitivity to an isolated relation or behavior under the chord stream that the deployed analysis pipeline supplies.

The practical consequence is simple. A generator can be highly responsive to a single, deliberately chosen chord change and still respond differently to the heterogeneous sequence emitted by a recognizer. Local probes should therefore be used to identify which harmonic relations matter, while complete replay should anchor claims about the behavior of the deployed chord-conditioned system.

This separation also makes robustness results easier to interpret. A large local effect establishes sensitivity to a named musical intervention, such as a relative-root change. A small replay distance establishes fidelity to the recognizer-conditioned operating case. Reporting both quantities disentangles mechanistic sensitivity from operating behavior and prevents a concentrated probe from being mistaken for the deployment condition it does not reproduce. Support-and-profile matching serves as a controlled intermediate condition: it retains intervention control while matching the temporal and relational structure that drives replay.

Code and derived metric tables are available in the public repository:
`github.com/Viwennnnnn/local-chord-corruption-replay`.

7. CONCLUSION

This study shows that a central four-second chord corruption is not a reduced form of complete recognizer replay. Under matched tracks, seeds, contexts, and scoring windows, the local tritone magnified chord-condition propagation on 29 of 30 tracks. Matching support and relation composition closed most of the gap across CNN–CRF and DeepChroma+CRF recognizer paths. The control sequence is a fundamental component of the evaluation, not a neutral carrier for a chord-error rate.

Robustness in analysis-conditioned generation depends on the complete control trajectory: support determines where the generator is challenged, and relation composition determines the harmonic nature of that challenge.

8. REFERENCES

[1] Chris Donahue, Antoine Caillon, Adam Roberts, Ethan Manilow, Philippe Esling, Andrea Agostinelli, Mauro Verzetti, Ian Simon, Olivier Pietquin, Neil Zeghidour, and Jesse Engel, "Singsong: Generating musical accompaniments from singing," 2023.

[2] Jianyi Chen, Wei Xue, Xu Tan, Zhen Ye, Qifeng Liu, and Yike Guo, "Fastsag: Towards fast non-autoregressive singing accompaniment generation," 2024.

[3] Fang-Duo Tsai, Yi-An Lai, Fei-Yueh Chen, Hsueh-Wei Fu, Li Chai, Wei-Jaw Lee, Hao-Chung Cheng, and Yi-Hsuan Yang, "Midi-informed singing accompaniment generation in a compositional song pipeline," 2026.

[4] Shuochen Gao, Shun Lei, Fan Zhuo, Hangyu Liu, Feng Liu, Boshi Tang, Qiaochu Huang, Shiyin Kang, and Zhiyong Wu, "An end-to-end approach for chord-conditioned song generation," 2024.

[5] Junan Zhang, Yunjia Zhang, Xueyao Zhang, and Zhizheng Wu, "Anyaccomp: Generalizable accompaniment generation via quantized melodic bottleneck," in *ICASSP 2026 – 2026 IEEE International Conference on Acoustics, Speech and Signal Processing (ICASSP)*, 2026, pp. 14812–14816.

[6] Ang Lv, Xu Tan, Peiling Lu, Wei Ye, Shikun Zhang, Jiang Bian, and Rui Yan, "GETMusic: Generating any music tracks with a unified representation and diffusion framework," 2023.

[7] Zhiqing Hong, Rongjie Huang, Xize Cheng, Yongqi Wang, Fuming You, Ruiqi Li, Zhou Zhao, and Zhimeng Zhang, "Text-to-song: Towards controllable music generation incorporating vocals and accompaniment," 2024.

[8] Ruiqi Li, Zhiqing Hong, Yongqi Wang, Lichao Zhang, Rongjie Huang, Siqi Zheng, and Zhou Zhao, "Accompanied singing voice synthesis with fully text-controlled melody," 2024.

[9] Shih-Lun Wu, Chris Donahue, Shinji Watanabe, and Nicholas J. Bryan, "Music ControlNet: Multiple time-varying controls for music generation," *IEEE/ACM Transactions on Audio, Speech, and Language Processing*, vol. 32, pp. 2692–2703, 2024.

[10] Jongmin Jung, Andreas Jansson, and Dasaem Jeong, "MusicGen-Chord: Advancing music generation through chord progressions and interactive web-UI," 2024.

[11] Jade Copet, Felix Kreuk, Itai Gat, Tal Remez, David Kant, Gabriel Synnaeve, and Yossi Adi, "Simple and controllable music generation," 2023.

[12] Christopher Harte, Mark B. Sandler, Samer A. Abdallah, and Emilia Gömez, "Symbolic representation of musical chords: A proposed syntax for text annotations," in *Proceedings of the 6th International Society for Music Information Retrieval Conference*, 2005, pp. 66–71.

[13] Johan Pauwels and Geoffroy Peeters, "Evaluating automatically estimated chord sequences," in *2013 IEEE International Conference on Acoustics, Speech and Signal Processing*, 2013, pp. 749–753.

[14] Matt McVicar, Raul Santos-Rodriguez, Yizhao Ni, and Tijl De Bie, "Automatic chord estimation from audio: A review of the state of the art," *IEEE/ACM Transactions on Audio, Speech, and Language Processing*, vol. 22, no. 2, pp. 556–575, 2014.

[15] Johan Pauwels, Ken O'Hanlon, Emilia Gómez, and Mark B. Sandler, "20 years of automatic chord recognition from audio," in *Proceedings of the 20th International Society for Music Information Retrieval Conference*, 2019, pp. 54–63.

[16] Laurent Oudre, Yves Grenier, and Cédric Févotte, "Template-based chord recognition: Influence of the chord types," in *Proceedings of the 10th International Society for Music Information Retrieval Conference*, 2009, pp. 153–158.

[17] Tristan Carsault, Jérôme Nika, and Philippe Esling, "Using musical relationships between chord labels in automatic chord extraction tasks," in *Proceedings of the 19th International Society for Music Information Retrieval Conference*, 2018, pp. 18–25.

[18] Katherine M. Kinnaird and Brian McFee, "Automatic hierarchy expansion for improved structure and chord evaluation," *Transactions of the International Society for Music Information Retrieval*, vol. 4, no. 1, pp. 81–92, 2021.

[19] Yiming Wu and Wei Li, "Automatic audio chord recognition with MIDI-trained deep feature and BLSTM–CRF sequence decoding model," *IEEE/ACM Transactions on Audio, Speech, and Language Processing*, vol. 27, no. 2, pp. 355–366, 2019.

[20] Filip Korzeniowski and Gerhard Widmer, "Feature learning for chord recognition: The deep chroma extractor," in *Proceedings of the 17th International Society for Music Information Retrieval Conference*, 2016, pp. 37–43.

[21] Sebastian Böck, Filip Korzeniowski, Jan Schlüter, Florian Krebs, and Gerhard Widmer, "madmom: A new python audio and music signal processing library," in *Proceedings of the 24th ACM International Conference on Multimedia*, 2016, pp. 1174–1178.

[22] Meinard Müller and Sebastian Ewert, "Chroma toolbox: MATLAB implementations for extracting variants of chroma-based audio features," in *Proceedings of the 12th International Society for Music Information Retrieval Conference*, 2011, pp. 277–282.

[23] Brian McFee, Colin Raffel, Dawen Liang, Daniel P. W. Ellis, Matt McVicar, Eric Battenberg, and Oriol Nieto, "librosa: Audio and music signal analysis in python," in *Proceedings of the 14th Python in Science Conference*, 2015, pp. 18–24.

[24] Zafar Rafii, Antoine Liutkus, Fabian-Robert Stöter, Stylianos Ioannis Mimilakis, and Rachel Bittner, "MUSDB18-HQ: An uncompressed version of MUSDB18," 2019.